ResearchGate

See discussions, stats, and author profiles for this publication at: https://www.researchgate.net/publication/341666050

Method for Detection of Meteotsunami Propagation in the Yellow Sea: Reported Cases

Conference Paper *in* Journal of Coastal Research · June 2020

DOI: 10.2112/SI95-220.1

CITATIONS
3

READS
36

6 authors, including:



Myung-Seok Kim
Korea Polar Research Institute (KOPRI)
22 PUBLICATIONS **91** CITATIONS
SEE PROFILE



Hyunmin Eom
Korea Meteorological Administration
13 PUBLICATIONS **49** CITATIONS
SEE PROFILE



Sung Hyup You
Korea Meteorological Administration
36 PUBLICATIONS **317** CITATIONS
SEE PROFILE



Seung Buhm Woo
Inha University
108 PUBLICATIONS **874** CITATIONS
SEE PROFILE

All content following this page was uploaded by Myung-Seok Kim on 06 September 2022.

The user has requested enhancement of the downloaded file.

Journal of Coastal Research	SI	95	1134–1139	Coconut Creek, Florida	2020

Method for Detection of Meteotsunami Propagation in the Yellow Sea: Reported Cases

Myung-Seok Kim[†], Hyunmin Eom[‡], Eun-Pyo Lim[§], Chan-Kyu Lee[††], Sung Hyup You[‡], and Seung-Buhm Woo[†*]

[†]Department of Oceanography
Inha University
Incheon, Republic of Korea

[‡]Marine Meteorology Division
Korea Meteorological Administration Seoul, Republic of Korea

[§]Marine Division
Sekwang Engineering
Seoul, Republic of Korea

[††]Observation Division
Korea Hydrography and Research Association
Seoul, Republic of Korea

www.cerf-jcr.org

www.JCRonline.org

ABSTRACT

Kim, M.-S.; Eom, H.; Lim, E.-P.; Lee, C.-K.; You, S.H., and Woo, S.-B., 2020. Method for detection of meteotsunami propagation in the Yellow Sea: Reported cases. *In:* Malvárez, G. and Navas, F. (eds.), *Global Coastal Issues of 2020*. *Journal of Coastal Research*, Special Issue No. 95, pp. 1134–1139. Coconut Creek (Florida), ISSN 0749-0208.

A new method for the detection of meteotsunami propagation using tide gauge data is described. This method is aimed to prevent disasters caused by meteotsunamis approaching from an unexpected direction. Three reported meteotsunami cases (31 March 2007, 4 May 2008, and 26 April 2011) in the Yellow Sea were analyzed to confirm the adequacy of the proposed propagation algorithm. In the March 31 case, the meteotsunamis propagated eastward at a speed of about 23.8-10.4 m/s from the WNW direction. On May 4, 2008, the meteotsunamis moved toward the accident area from the southwest coast of Korea at a speed of about 27.8-10.9 m/s. The meteotsunamis of 26 April 2011 were focused on the southern part of the Yellow Sea, especially at DaeHeuksando (DH) harbor. In comparison with the result of previous studies, the propagation results calculated using the proposed algorithm showed a similar propagation pattern and a reasonable endpoint toward the point where the accident occurred. By using data from the existing tide gauges, this method for the detection of a meteotsunami propagation can track propagation patterns that vary with time and space. It is expected to be useful when developing a meteotsunami warning system.

ADDITIONAL INDEX WORDS: *Meteotsunami, propagation algorithm, reported cases.*

INTRODUCTION

At noon on Sunday, May 4, 2008, sudden abnormal waves hit the west coast of Korea. The unexpected waves swept fishermen from breakwaters near BoRyeong (BR), and nine people were killed (Choi and Lee, 2009). Similar phenomena were also reported on March 31, 2007, and April 26, 2011, causing substantial damage to property and human lives. It was found that the sudden waves in the Yellow Sea were caused by meteotsunamis generated by the propagation of pressure jumps. A meteotsunami is defined as significantly amplified sea-level oscillations due to Proudman resonance (Proudman, 1929), which occurs when the velocity of a pressure jump matches that of a shallow-water wave during the propagation process (Monserrat, Vilibić, and Rabinovich, 2006). Therefore, when considering methods for coastal disaster prevention, it is important to analyze where the meteotsunami propagated from and where it was concentrated.

The propagation direction generally depends on the arrival time of the meteotsunami. As shown in Table 1, the arrival time analysis of the meteotsunamis is classified into four methods based on previous studies. It is also classified into methods using the absolute criterion and methods using the relative criterion depending on whether the background noise at each observation point is considered.

In previous studies, when analyzing the propagation direction of the reported meteotsunami cases, the ocean model was simulated using the propagation scenarios of the linear pressure jump, which were derived from meteorological observations (Cho *et al.*, 2013; Choi and Lee, 2009; Eom *et al.*, 2012). However, the previous propagation analyses required considerable amounts of time and computational resources when developing a real-time meteotsunami monitoring system. Moreover, it is not possible to analyze the variations in meteotsunami propagation concerning time and space such as that in the case of storm tracks. Our study has two main objectives: (i) to provide a direct method for the detection of meteotsunami propagation based on tidal observations, and (ii) to identify the propagation pattern of the reported meteotsunami cases using the suggested method.

METHODS

The selected criterion for meteotsunami arrival time and a new method for the propagation were suggested in this section.

Criteria for Arrival Time of Meteotsunami

Tide gauge records with a sampling interval of 1 min were used in this study. As indicated by the red squares in Figure 1, five tide

DOI: 10.2112/SI95-220.1 received 31 March 2019; accepted in revision 13 February 2020.
*Corresponding author: sbwoo@inha.ac.kr
©Coastal Education and Research Foundation, Inc. 2020

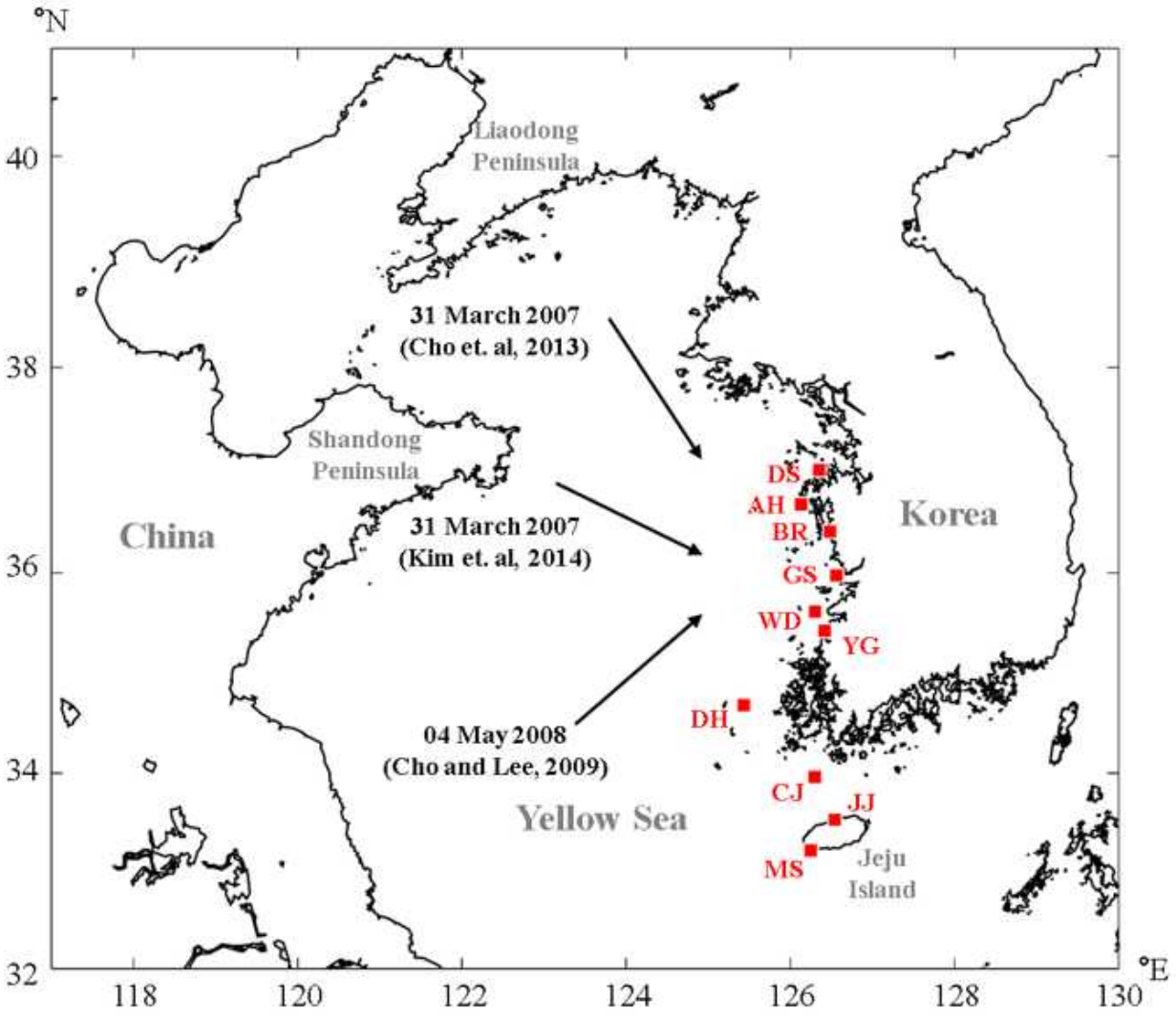


Figure 1. Location of the study area, showing the locations of the tide gauges (red squares) and propagation direction (black arrows) of the reported meteotsunami cases.

Table 1. *Preliminary studies on the criteria for meteotsunami arrival time.*

Method	Types of Criteria	Criteria for Arrival Time	Preliminary Studies
Method #1	Absolute threshold	30 cm, wave height	Rabinovich and Monserrat (1996)
Method #2	Relative threshold	3-4 sigma, wave amplitude	Monserrat, Vilibić, and Rabinovich (2006)
Method #3	Relative threshold	Maximum wave amplitude	Kim *et al.* (2017)
Method #4	Combined threshold	Method #1 + Method #2	Monserrat, Vilibić, and Rabinovich (2006)

gauges were located on the west coast of the Korean Peninsula: DaeSan (DS), AnHeung (AH), BoRyeong (BR), GunSan (GS), and YeongGwang (YG). The other tide gauges were deployed in islands near the Korean Peninsula: WiDo (WD), DaeHeuksando (DH), ChuJado (CJ), JeJu (JJ), and MoSeulpo (MS).

For meteotsunami arrival time analysis, the sea-level oscillations corresponding to the meteotsunami frequency range (Monserrat, Vilibić, and Rabinovich, 2006) were high-pass filtered with a wavelet filter based on Morlet window (Torrence and Compo, 1998). Since the meteotsunami cases analyzed in this study were already reported cases, it was not necessary to determine whether the meteotsunamis had occurred. However, to find the tide gauges where the high-intensity meteotsunami waves were concentrated, the lower limit was set to distinguish the presence or absence of meteotsunamis at each tide gauge. Therefore, the tide gauges where the maximum amplitude of the sea-level oscillations did not

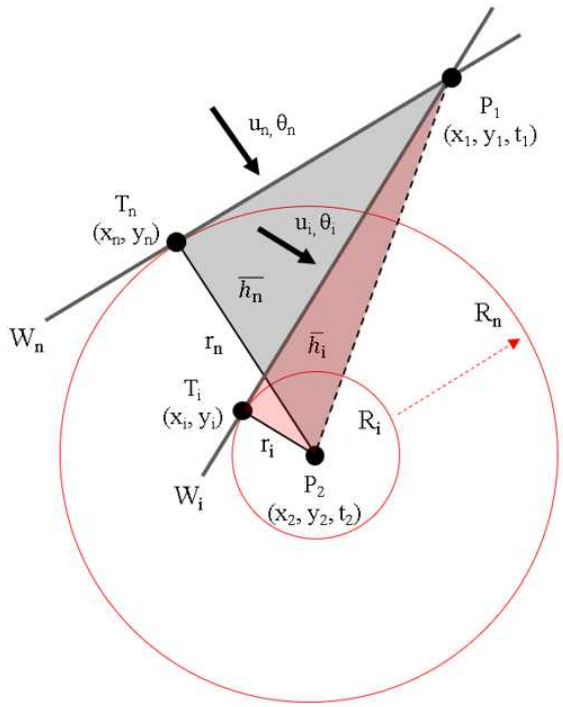


Figure 2. Method for detection of meteotsunami propagation.

exceed the lower limit (10 cm) were considered as the tide gauges where a meteotsunami did not occur. As shown by the red circles in Figure 3, the time when the maximum amplitude occurred was determined as the arrival time of the meteotsunami. In this study, we simultaneously used the absolute and relative thresholds (Monserrat, Vilibić, and Rabinovich, 2006) for determining the arrival time (Method #1 and Method #3 in Table 1).

Method for Detection of Meteotsunami Propagation

In Figure 2, P_1 and P_2 denote the locations where the meteotsunami arrived first and arrived next, respectively. It is assumed that the meteotsunami propagates in the form of a linear wave crest from P_1 to P_2. In the region representing the difference in arrival times at the two points ($\Delta t=t_2-t_1$), concentric circles centered on P_2 (R_i-R_n) with various radii (r_i-r_n) can be drawn sequentially.

The tangent lines from P_1 to the tangent points (T_i-T_n) on the concentric circles (R_i-R_n) represent the wave crest lines (W_i-W_n) of the meteotsunami propagating between P_1 and P_2. Since the meteotsunamis that have been reported so far propagated from the west, we chose a tangent point located relatively west. The speed of the wave crest line per concentric circle was calculated using Eq. (1).

$$u_{wi} = r_i / \Delta t \ , \tag{1}$$

Considering the ratio of the meteotsunami wavelength (λ) to water depth (h) in the Yellow Sea, the meteotsunami, which is characterized by a wavelength of about 10 to 100 km (Vilibić *et al.*,

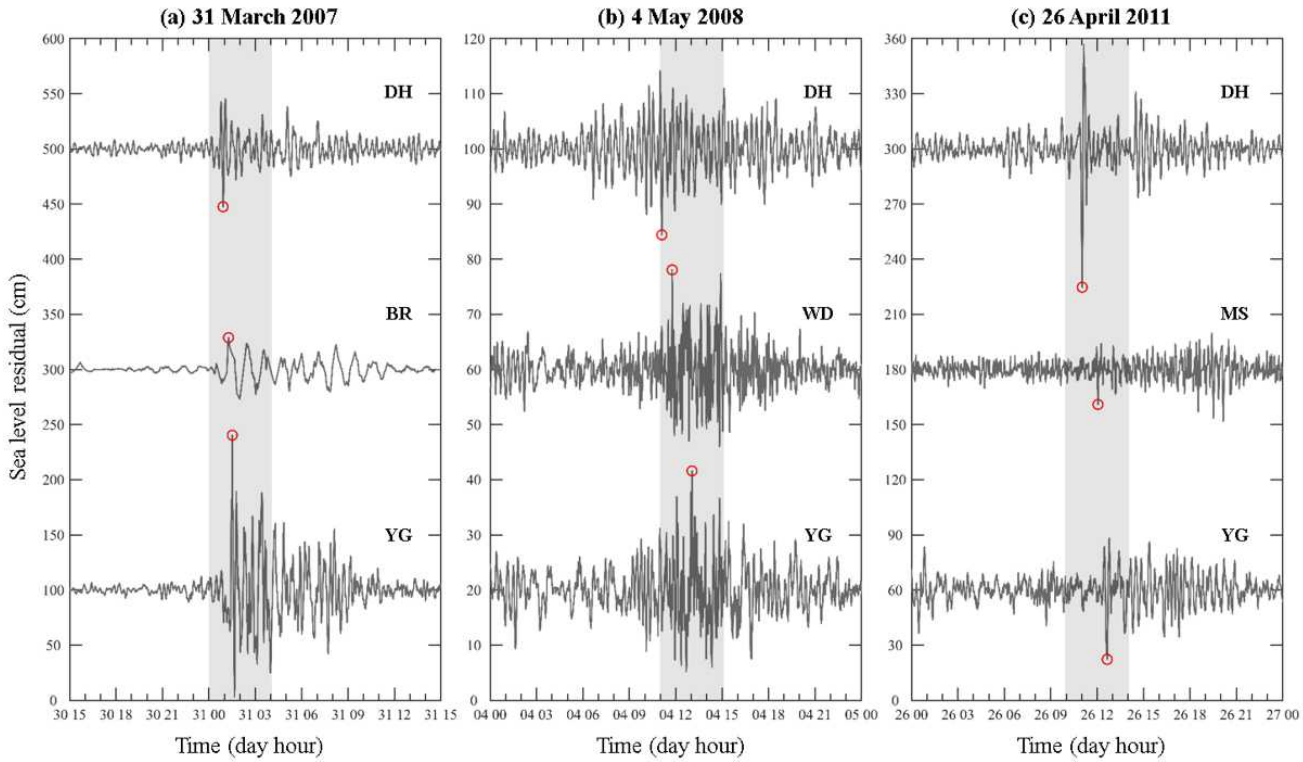


Figure 3. Filtered sea-level records (2-h) and arrival time (red circles) of the reported meteotsunami cases. (a) 31 March 2007 case, (b) 4 May 2008 case, and (c) 26 April 2011 case. The period used for the arrival time analysis (4-h) is highlighted by the gray-shaded area.

2016), in the Yellow Sea with a maximum depth of less than 100 m, is considered as a shallow water wave ($\lambda >> 20$ h). Therefore, the shallow water wave velocity (u_{ci}-u_{cn}) can be estimated using the mean depth of the triangle area (h_i-h_n) surrounded by the tangent points (T_i-T_n), P_1, and P_2 (Eq. (2)).

$$u_{ci} = \sqrt{g\overline{h_i}}\ , \tag{2}$$

The boundary of the triangle, which varies according to the position of the tangent point (T_i-T_n) is entirely dependent on the radius (r_i-r_n). As a result, based on Eq. (1) and Eq. (2), the propagation direction (θ_i-θ_n) and speed (u_i-u_n) of the meteotsunami are determined from the radius (r_i-r_n) of the concentric circles (R_i-R_n). By using Eq. (3), it is necessary to find the most reasonable radius (r_j) satisfying the minimum absolute difference (ε_j) between the meteotsunami speeds calculated using Eq. (1) and Eq. (2).

$$\varepsilon_j = \left| u_{wj} - u_{cj} \right|, \tag{3}$$

Then, the wave crest line (W_j), propagation direction (θ_j), and speed (u_j) of the meteotsunami between P_1 and P_2 can be calculated based on the determined radius (r_j) of the concentric circles (R_j). Using the same process described above, it is possible to analyze the meteotsunami propagation pattern for the observation points at which the wave arrives sequentially after P_1 and P_2.

RESULTS

The meteotsunami propagation of the reported cases was analyzed using the proposed method.

31 March 2007 Case

The meteotsunami case of 31 March 2007 is considered as the most powerful case among the reported cases. Tsunami-like oscillations were observed at most tide gages (Figure 3(a)). As the sea-level oscillations rapidly increased to the peak of the maximum amplitude and then decreased, it was easy to determine the arrival time of the meteotsunamis. In all the tide gauges, the maximum amplitude of the sea-level oscillations exceeded the minimum amplitude threshold of the meteotsunami (10 cm). The first meteotsunami arrived at AH, followed by DH, WD, BR, GS, DS, YG, CJ, JJ, and MS (Figure 4(a), Table 2). The sea-level oscillations propagated mainly from the WNW direction at the source point outside the Yellow Sea, and the calculated wave crest lines near the coast approached parallel to the shoreline.

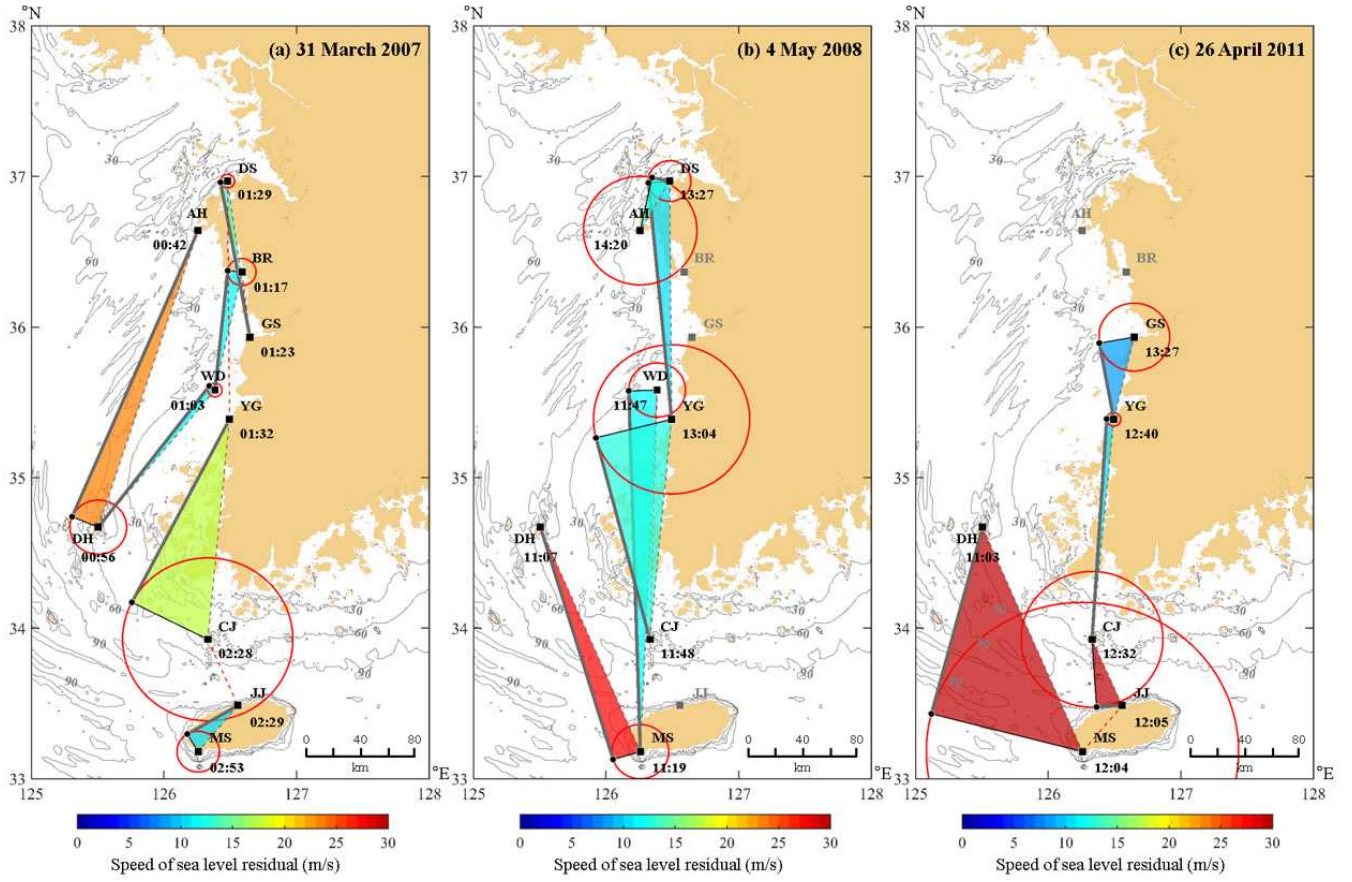


Figure 4. Propagation map and arrival time of the reported meteotsunami cases. (a) 31 March 2007 case, (b) 4 May 2008 case, and (c) 26 April 2011 case. Black squares indicate the tide gauges where the meteotsunami arrived. Tide gauges where the maximum amplitude of the meteotsunami is less than 10 cm are marked by gray squares. The thick gray lines indicate the wave crest line of the meteotsunamis, and the dashed gray lines indicate the line connecting one tide gauge to another. The color of the triangles indicates the speed of the meteotsunami in each region. The radius of each red circle is the distance that the sea-level oscillations can propagate, and the black lines indicate the determined line of the radius. The red dashed lines between two tide gauges indicate exception cases in which it was unable to find a solution for the propagation. The dashed gray lines are bathymetric contours (30, 60, and 90 m).

Table 2. *Order of arrival time, direction, and speed of the meteotsunami cases.*

Order of Arrival	Tide Gauge (P_1-P_2)	Direction (deg)	Speed (m/s)
	31 March 2007		
1	AH-DH	292.8	23.8
2	DH-WD	306.9	11.9
3	WD-BR	275.8	11.9
4	BR-GS	-	-
5	GS-DS	259.7	13.9
6	DS-YG	-	-
7	YG-CJ	297.0	17.9
8	CJ-JJ	-	-
9	JJ-MS	329.4	10.4
	4 May 2008		
1	DH-MS	253.3	27.8
2	MS-WD	268.2	11.9
3	WD-CJ	-	-
4	CJ-YG	255.7	12.1
5	YG-DS	264.7	10.9
6	DS-AH	192.0	12.6
	26 April 2011		
1	DH-MS	284.7	30.1
2	MS-JJ	-	-
3	JJ-CJ	356.3	30.9
4	CJ-YG	273.6	10.4
5	YG-GS	259.8	8.9

4 May 2008 Case

Compared to the other meteotsunami cases, the sea-level oscillations slowly increased to the maximum amplitude. Therefore, it was not easy to determine the arrival time based on criteria other than the maximum amplitude. As shown in Figure 4 (b), the first meteotsunami was detected at DH, and it propagated at a speed of 27.8-10.9 m/s from the WSW direction to the accident place near BR where the human casualties were reported (Table 2). Interestingly, sea-level oscillations less than 10 cm were observed at BR and GS near the accident place (gray squares in Figure 4(b)). From the locations of the first and last arrival points, it can be seen that the meteotsunami of 4 May 2008 propagated northward from the southern Yellow Sea.

26 April 2011 Case

As shown in Figure 4 (c), the meteotsunamis of 26 April 2011 were primarily concentrated at DH. Within a couple of minutes, the sea-level oscillations at DH reached a maximum wave height of about 1.5 m and were damped very rapidly (Figure 3(c)). DS and WD, which were the missing points during the period of observation, were excluded from the propagation analysis. The meteotsunami that first arrived at DH with a high speed of about 30 m/s propagated toward the west coast of the Korean Peninsula with a spatial scale of the wave crest line, which is limited to the southern Yellow Sea (Figure 4(c), Table 2). For tide gauges at MS and JJ, as the area between the two points was located on land, we cannot calculate the shallow water wave celerity of the meteotsunami (red dashed line in Figure 4(c)).

DISCUSSION

To confirm the accuracy of the propagation pattern calculated using the algorithm, it was compared with the propagation direction of the reported meteotsunami cases suggested in the previous study (black arrows in Figure 1 and Figure 4). Cho *et al.* (2013) assumed that the meteotsunami of 31 March 2007 propagated from the direction of NNW (from the Liaodong Peninsula to YG), by analyzing the propagation pattern of the pressure jump that caused the sea-level oscillations. Based on the synoptic weather analysis around the Yellow Sea and the meteorological model, Kim *et al.* (2014) suggested that the pressure disturbances and the sea-level oscillations passed over the Yellow Sea in the direction from the Shandong Peninsula to YG (WNW). In the previous studies, the propagation direction of the meteotsunamis was derived indirectly from the atmospheric data. Therefore, it was not possible to determine which propagation pattern is the reference solution. However, the calculated propagation of 31 March 2007 in this study was quite similar to that found by Kim *et al.* (2014) about the propagation pattern (speed, direction, and source point of the meteotsunami). Moreover, the spatial and temporal patterns of the calculated propagation for the meteotsunami of 4 May 2008 was coincident with the evolution of the atmospheric instability in the weather map and the radar imagery analyzed by Choi and Lee (2009).

It was possible to analyze the meteotsunami-track and spatial scale that changed with time and space using the propagation method. This propagation method may be useful when inversely estimating the propagation pattern of the pressure jump, which is responsible for the formation of the unexpected meteotsunami. In our future work, we will consider the tide level when a meteotsunami arrives. This is because the influence of the tide level on the water depth cannot be ignored in the case of the Yellow Sea, which is a macro-tidal environment.

CONCLUSIONS

A new method for detecting the propagation of meteotsunamis using the long-wave characteristics of the sea level oscillations was proposed. By applying the proposed propagation method to the reported meteotsunami cases of 31 March 2007, 4 May 2008, and 26 April 2011, it was confirmed that these meteotsunamis respectively propagated from the directions of WNW, WSW, and W, which were similar to the previous research results. This method can be used with a limited number of tide gauges. Therefore, it can be utilized as an early stage of research for the prevention of meteotsunami disasters in the Yellow Sea in a short time. Shortly, when operating a meteotsunami warning system in the Yellow Sea, this method is expected to be practically useful by deploying more tide gauges.

ACKNOWLEDGMENTS

This research was a part of the project titled ‘Improvements of ocean prediction accuracy using numerical modeling and artificial intelligence technology’, funded by the Ministry of Oceans and Fisheries, Korea. Additionally, this research was supported by Basic Science Research Program through the National Research Foundation of Korea (NRF) funded by the Ministry of Education (2019R1A6A3A13097301).

LITERATURE CITED

Choi, J.-Y. and Lee, D.-Y., 2009. Analysis of small-scale atmospheric pressure jumps related to the generation of abnormal extreme waves at Boryeong. *Ocean and Polar Research*, 31(4), 379-388.

Cho, K.-H.; Choi, J.-Y.; Park, K.-S.; Hyun, S.-K.; Oh, Y., and Park, J.-Y., 2013. A synoptic study on tsunami-like sea level oscillations along the west coast of Korea using an unstructured-grid ocean model. In: Conley, D.C., Masselink, G., Russell, P.E. and O'Hare, T.J. (eds.), *Proceedings 12th International Coastal Symposium (Plymouth, England)*, *Journal of Coastal Research*, (65), 678-683.

Eom, H.-M.; Seung, Y.H.; Woo, S.-B., and You, S.-H., 2012. Analysis of abnormal wave at the west coast on 31 March 2007. *Journal of Korean Society of Coastal Ocean Engineers*, 24(3), 217-227.

Kim, H.; Kim, Y.-K.; Woo, S.-B., and Kim, M.-S., 2014. Atmospheric analysis on the meteo-tsunami case occurred on 31 March 2007 at the Yellow Sea of South Korea. *Journal of Environmental Science International*, 23(12), 1999-2014.

Kim, M.-S.; Kim, H.; Kim, Y.-K.; You, S.-H.; Eom, H.-M., and Woo, S.-B., 2017. Determination of Accurate Arrival Time of Meteotsunami Event in Yellow Sea. In: Lee, J.L.; Griffiths, T.; Lotan, A.; Suh, K.-S., and Lee, J. (eds.), *The 2nd International Water Safety Symposium*, *Journal of Coastal Research*, (79), 149-153.

Monserrat, S.; Vilibić, I., and Rabinovich, A.B., 2006. Meteotsunamis: Atmospherically induced destructive ocean waves in the tsunami frequency band. *Natural Hazards Earth System Sciences*, 6, 1035-1051.

Proudman, J., 1929. The effects on the sea of changes in atmospheric pressure. *Geophysical Journal International*, 2(4), 197-209.

Rabinovich, A.B. and Monserrat, S., 1996. Meteorological tsunamis near the Balearic and Kuril Islands: Descriptive and statistical analysis. *Natural Hazards*, 13(1), 55-90.

Torrence, C. and Compo, G.P., 1998. A practical guide to wavelet analysis. *Bulletin of the American Meteorological Society*, 79, 61-78.

Vilibić, I.; Šepić, J.; Rabinovich, A.B., and Monserrat, S., 2016. Modern approaches in meteotsunami research and early warning. *Frontiers in Marine Science*, 3(57), 1–7.

View publication stats